New Phytologist

The velamen protects photosynthetic orchid roots against UV-B damage, and a large dated phylogeny implies multiple gains and losses of this function during the Cenozoic

Guillaume Chomicki[1]*, Luc P. R. Bidel[2]*, Feng Ming[3,4]*, Mario Coiro[5], Xuan Zhang[3,4], Yaofeng Wang[3,4], Yves Baissac[6], Christian Jay-Allemand[6] and Susanne S. Renner[1]

[1]Systematic Botany and Mycology, Department of Biology, University of Munich (LMU), Munich 80638, Germany; [2]INRA, UMR AGAP, Montpellier, France; [3]State Key Laboratory of Genetic Engineering, Institute of Genetics, Shanghai 200433, China; [4]Institute of Plant Biology, School of Life Science, Fudan University, 220 Handan Road, Shanghai 200433, China; [5]Institute of Agricultural Sciences, Plant Biochemistry, ETH Zurich, 8092 Zurich, Switzerland; [6]UMR DIADE (UM2/IRD), SMART Team, University of Montpellier 2, Place Eugene Bataillon, Montpellier F-34 095, France

Author for correspondence:
Guillaume Chomicki
Tel: +49 89 17861 285
Email: guillaume.chomicki@gmail.com

Received: *9 July 2014*
Accepted: *8 September 2014*

New Phytologist (2015) **205:** 1330–1341
doi: 10.1111/nph.13106

Key words: chalcone synthase, dated phylogeny, epiphytes, flavonoids, gene duplication, orchids, UV-B, velamen.

Summary

• UV-B radiation damage in leaves is prevented by epidermal UV-screening compounds that can be modulated throughout ontogeny. In epiphytic orchids, roots need to be protected against UV-B because they photosynthesize, sometimes even replacing the leaves. How orchid roots, which are covered by a dead tissue called velamen, avoid UV-B radiation is currently unknown.

• We tested for a UV-B protective function of the velamen using gene expression analyses, mass spectrometry, histochemistry, and chlorophyll fluorescence in *Phalaenopsis* × *hybrida* roots. We also investigated its evolution using comparative phylogenetic methods.

• Our data show that two paralogues of the chalcone synthase (*CHS*) gene family are UV-B-induced in orchid root tips, triggering the accumulation of two UV-B-absorbing flavonoids and resulting in effective protection of the photosynthetic root cortex. Phylogenetic and dating analyses imply that the two *CHS* lineages duplicated *c.* 100 million yr before the rise of epiphytic orchids.

• These findings indicate an additional role for the epiphytic orchid velamen previously thought to function solely in absorbing water and nutrients. This new function, which fundamentally differs from the mechanism of UV-B avoidance in leaves, arose following an ancient duplication of *CHS*, and has probably contributed to the family's expansion into the canopy during the Cenozoic.

Introduction

With over 27 600 species (Zotz, 2013), vascular epiphytes are a key element of rainforest canopies. Epiphytic orchids account for 68% (19 000 species) of these epiphytes (Zotz, 2013). Although epiphytes often grow in humid environments, their supply of water and nutrients tends to be highly uneven (Laube & Zotz, 2003). Accordingly, epiphytes have characteristic adaptations, for example crassulacean acid metabolism (CAM) photosynthesis (Winter *et al.*, 1983; Crayn *et al.*, 2004; Silvera *et al.*, 2009), leaf rosette tanks for storing water (Benzing, 2008; Givnish *et al.*, 2014), and myrmecotrophy, where ants supply nitrogen to their host plant (Huxley, 1978; Gay, 1993; Gegenbauer *et al.*, 2012). In orchids, CAM photosynthesis is strongly associated with the epiphytic habit (Silvera *et al.*, 2009), and many epiphytic orchids also have succulent leaves. While some epiphytic lineages, such as bromeliads, have reduced their root system to an anchoring function (Benzing, 2000), most orchid species evolved photosynthetic roots, a way to increase photosynthetic surface and hence carbon gain (Kwok-ki *et al.*, 1983). Some 300 epiphytic orchid species rely exclusively upon root photosynthesis for carbon gain (Cockburn *et al.*, 1985; Chomicki *et al.*, 2014).

In addition to an uneven water supply and nutrient stress, an important stress factor in epiphytes is high and fluctuating irradiation, including harmful UV-B (280–320 nm; Canham *et al.*, 1990; Flint & Caldwell, 1998). UV-B radiation is a major hazard for living organisms exposed to sunlight, causing DNA mutations, plasma membrane lipid peroxidation and photosynthetic machinery degradation in plant cells (Jansen *et al.*, 1998; Sinha & Häder, 2002; Bray & West, 2005). In vascular plant leaves, accumulation of UV-B screening compounds – such as flavonoids – in the epidermis provides efficient protection and can

*These authors contributed equally to this work.

screen out over 95% of the incident UV-B radiation (Caldwell *et al.*, 1983). Mutants of the chalcone synthase (*CHS*) gene, which encodes an enzyme that initiates the flavonoid biosynthetic pathway, are hypersensitive to UV radiation (Li *et al.*, 1993), indicating the pivotal role of flavonoids in UV-B photoprotection. Carbon investment in flavonoids for photoprotection can be modulated throughout leaf ontogeny (Burchard *et al.*, 2000; Bidel *et al.*, 2007), permitting dynamic acclimation to a fluctuating ambient UV-B irradiance. But how do photosynthetic orchid roots cope with UV-B radiation? This question is especially puzzling as a spongy tissue, the velamen, consisting of dead cells, covers the roots of all epiphytic orchids.

Through an approach integrating histocytochemistry, metabolic and gene expression profiling, chlorophyll fluorescence and phylogenetic comparative methods, we ask the following questions: (1) How do the photosynthetic roots of epiphytic orchids acclimate to UV-B radiation given that a dead tissue covers them? We specifically test the hypothesis that the velamen accumulates UV-B screening compounds before its maturation, that is, in the growing root apex. (2) Is differential expression among duplicated *CHS* genes involved in such a protective mechanism? If so, when did the duplication(s) occur as compared to the time of origin of epiphytic orchids? (3) Finally, by tracing the evolution of habit in orchids, we ask: when and how many times, at a minimum, did root UV-B avoidance function arise or become lost (again)?

Materials and Methods

Plant material

Plant material was collected from cultivated specimens at the Munich Botanical Garden or near Gueret, France. Herbarium vouchers have been deposited in the Munich herbarium ([M]). *Arpophyllum giganteum* Hartw. ex Lindl. (G. Chomicki 6 [M]), *Vanilla planifolia* Jacks. ex Andrews (G. Chomicki 3 [M]), *Cypripedium kentuckiense* C.F. Reed (G. Chomicki 4 [M]), *Dendrophylax lindenii* (G. Chomicki 5 [M]) and *Dactylorhiza fuchsii* (Druce) Soó (G. Chomicki 7 [M]). *Phalaenopsis* × *hybrida* cultivar 'Aphrodite' (G. Chomicki 8 [M]) was purchased from local nurseries.

Plant growth conditions and stress treatment

Phalaenopsis × *hybrida* cultivar 'Aphrodite' plants were grown in pots kept at 24°C under a 16-h photoperiod. Plants with at least four mature leaves were used for UV treatment. For both liquid chromatography–mass spectrometry (LC-MS) and qRT-PCR experiments, UV-B treatment was performed at an intensity of 250 $\mu W\,cm^{-2}$ and a wavelength of 312 nm with a 30-W lamp (Uvitec, Cambridge, UK), reflecting the UV irradiance that orchid roots can receive in their natural environment. During the treatments, only selected roots were exposed to UV-B radiation, and the rest of the plant was protected under thin foil. For LC-MS experiments, single UV-B doses of 12 h were given; qRT-PCR was carried out after 4, 8, and 12 h, and in addition to partitioning the sample into upper and lower root regions, the apical region (the first 1 cm of the root) was sampled separately from the rest of the root. Each sample consisted of 100 mm^2 of tissue stripped under a binocular microscope, and the area was evaluated using binocular images.

Microscopy, flavonoid histolocalization and image analysis

Epifluorescence microscopy was carried out on a Nikon Eclipse E600 epifluorescence microscope fitted to a Nikon Ds-Fi 1 camera or a Leica DMR microscope equipped with a KAPPA-CCD camera. A Nikon B2-A filter (excitation spectrum 450–480 nm) was used to detect flavonoid fluorescence. For the same root section, successive immersions in distilled water and in aqueous diphenyl boric acid-2-aminoethyl ester (DPBA) solution (Sheahan & Rechnitz, 1992) were performed for comparing tissue autofluorescence and flavonoid-enhanced fluorescence after DPBA complexation. Image analysis was performed in ImageJ (http://rsb.info.nih.gov/ij). The intensity of flavonoid fluorescence was evaluated by plotting intensity profiles (as grey values) of DPBA-stained sections and subtracting the values obtained for autofluorescence observed in the same sections (see Fig. 1 and Supporting Information Fig. S1).

High-performance liquid chromatography–mass spectrometry (HPLC-MS) flavonoid characterization

For each sample, *c.* 100 mm^2 of velamen was stripped and immediately immerged in extraction solution. In a pilot experiment for the project, we sought to identify phenolic compounds induced by UV-B radiation. We found only two significantly induced flavonoids, which were also the two major phenolics identified in the mature velamen, and we thus focused on these two compounds in this study. The flavonoid profile of the different tissues of a light-grown *Phalaenopsis* × *hybrida* leaf is shown in Fig. S2. The extraction solution consisted of methanol/water (70/30, v/v) acidified with 0.1% HCl. 5-*O*-methoxyflavone, which is not synthesized by this plant species (*Phalaenopsis* × *hybrida*), was added and used as an internal standard. Samples were frozen in liquid nitrogen, sonicated for 10 min in cold water and then stored at −20°C. Twenty microlitres of the centrifuged solution was injected in LC-MS.

Chromatographic separation was performed on an XTerra MS C_{18} column (3.5 µm particle size; 2.1 × 100 mm) (Gecko 2000; Cluzeau Info Labo, Sainte-Foy-La-Grande, France) heated to 40°C. A binary mobile phase gradient was delivered at a total flow rate of 210 $\mu l\,min^{-1}$ using an HPLC pump (Waters 1525µ; Waters, Manchester, UK). The phase gradient was composed of permuted water (solvent A) and acetonitrile (solvent B), both phases acidified with 0.1% (v/v) formic acid in order to minimize the ionization of phenolics (pH *c.* 3.0). A Micromass ZQ ESCi multimode ionization mass spectrometer (Micromass Ltd, Manchester, UK) equipped with an electrospray ionization ion source (ZSpray MKII) was used. Source and capillary were heated to 90 and 450°C, respectively, and capillary voltage was set to 2.5 kV. Nitrogen was used as the desolvatation gas ($400\,l\,h^{-1}$) and cone gas ($50\,l\,h^{-1}$). In a first step, spectra were recorded in the full scan

New Phytologist

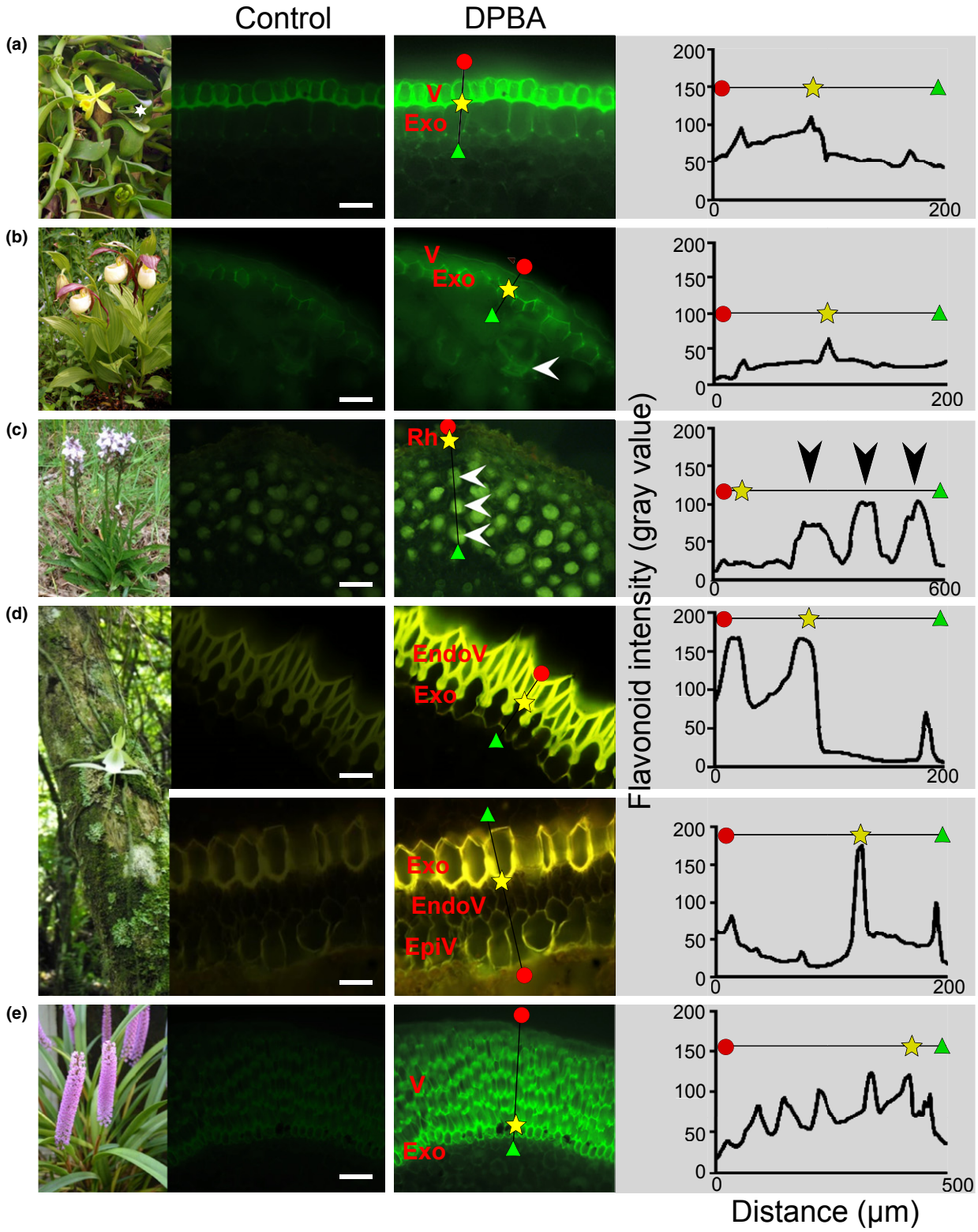

Fig. 1 Distribution of flavonoids in orchid roots. (a) *Vanilla planifolia*. (b) *Cypripedium kentuckiense*. (c) *Dactylorhiza fuchsii*. (d) *Dendrophylax lindenii*. The lower left panel shows a close-up of the photosynthetic root with the pneumatodes (arrowhead), through which gas exchange occurs. (e) *Arpophyllum giganteum*. Panels on the right show flavonoid intensity as the ratio of diphenyl boric acid-2-aminoethyl ester (DPBA)-stained fluorescence to autofluorescence along the axis shown in the photograph. The start marks the exodermis outer wall. Bars: (a) 80 μm; (b) 100 μm; (c) 150 μm; (d, upper panel) 70 μm; (d, lower panel) 40 μm; (d, root) 0.3 cm; (e) 120 μm. EndoV, Endovelamen; EpiV, Epivelamen; Exo, Exodermis; Rh, Rhizodermis.

mode over the *m/z* 50–1200 range, both in negative and positive modes. Absorbance spectra over the range of 210–800 nm were acquired using a Waters 996 photodiode array detector. Absorbance and mass spectra were analysed using MassLynx 3.5 software (Micromass Ltd). Saponarin standards were used to confirm flavonoid identity (Extrasynthese, Genay, France).

Chlorophyll fluorescence analysis

A modulated chlorophyll *a* (Chl*a*) fluorescence analysis was performed on dark-adapted roots (over a 40-min period), using a portable PAM2000 fluorometer connected to its clip (Heinz Walz GmbH, Pfullingen, Germany). To test whether the velamen effectively protects the photosynthetic root cortex, we measured the quantum yield of light-grown roots with well-developed velamen before and after a 4-h UV-B irradiation at 312 nm and 250 μW cm^{-2}, with the expectation that, if the velamen does not protect the root cortex, the quantum yield should decrease in UV-B-treated roots. The maximum efficiency of photosystem II (PSII) was calculated as $F_v/F_m = (F_m - F_0)/F_m$, where F_v is the variable fluorescence and F_m is the maximum fluorescence of the roots. The minimum fluorescence, F_0, was measured using a modulated light pulse < 1 μmol m^{-2} s^{-1}. F_m and F'_m were determined at 20 kHz using a 0.8 s^{-1} saturating light pulse of white light at 8000 μmol m^{-2} s^{-1}.

qRT-PCR expression analyses of *PhCHS3*, *PhCHS4* and *PhCHS5*

Total RNA was extracted using RNAiso Plus (Takara; http://www.takara.com.cn) according to the manufacturer's instructions. Complementary DNA was produced using the PrimeScript™ RT reagent Kit (Takara). Quantitative PCR (qPCR) reactions were performed using gene-specific primers in a total volume of 10 μl with SYBR®Premix Ex Taq™ II (Takara) on a MyiQ™2 (Bio-Rad) apparatus under the following conditions: pre-incubation at 95°C for 3 min and 40 cycles of 95°C for 10 s and 55°C for 30 s, with melting curves according to the manufacturer's recommendations. The fold change of *PhCHS* genes was calculated using the comparative cycle threshold method (Livak & Schmittgen, 2001) following normalization based on *PhActin* (AF246714.1) expression. Table S1 reports the pairwise correlation statistics of the different *PhCHS* gene expression patterns. The specific primers used for *PhCHS3*, *PhCHS4*, *PhCHS5* and *PhActin* are listed in Table S2.

Phylogenetic analysis of chalcone synthase

A total of 148 CHS-like protein sequences were downloaded from GenBank (http://www.ncbi.nlm.nih.gov) and the 1000 genome project (http://onekp.com/project.html) (see accession numbers in Fig. S3). Sequences were aligned using MAFFT v. 7.0 (Katoh & Standley, 2013) under default settings and further edited by eye in Mesquite v. 2.75 (Maddison & Maddison, 2011). The amino acid substitution model best fitting our data was LG + G, as determined according to the Akaike information criterion (AIC) criterion, implemented in ProtTest (Darriba *et al.*, 2011). Maximum likelihood (ML) inference relied on RAxML v. 7.0 (Stamatakis *et al.*, 2008) with 100 ML bootstrap replicates.

Molecular clock dating of the Orchidaceae

To generate a dated phylogeny of the Orchidaceae, we downloaded 1144 sequences from GenBank (http://www.ncbi.nlm.nih.gov) representing four plastid and nuclear markers (*matK*, *rbcL*, ITS and *trnL-trnF*) and 340 species (335 orchids plus five outgroup species; Table S3). Phylogeny tips were handled using Phyutility (Smith & Dunn, 2008). Sequences of each marker were aligned using MAFFT v. 7.0 (Katoh & Standley, 2013) with the default settings (*rbcL* and *matK*) and then again with a Q-INS approach, taking into account secondary RNA structure, followed by editing by eye in Mesquite v. 2.75 (Maddison & Maddison, 2011). For ITS and *trnL-trnF* only, poorly aligned regions were removed using Gblocks (Castresana, 2000), under low-stringency settings; for ITS, poorly aligned regions were removed manually. All missing data, including terminal gaps, were coded as 'N'. In the absence of major, statistically supported (i.e. Bootstrap (BS) > 80%) topological incongruence between the plastid and the nuclear data, matrices were concatenated to form an alignment of 4245 nucleotides. ML inference relied on the GTR + G substitution model, with six gamma rate categories and four unlinked data partitions.

The relationships of Vanilloideae and Cypripedioideae were not resolved by these data (Fig. S4), as had also been the case in earlier analyses (Cameron *et al.*, 1999; Freudenstein & Chase, 2001; Freudenstein *et al.*, 2004; Górniak *et al.*, 2010). We therefore constructed a matrix with 26 species from all five orchid subfamilies, plus six outgroups using seven markers (*matK*, *rbcL*, ITS, *trnL-trnF*, *18S ribosomal RNA* (*18S*), *xanthine dehydrogenase* (*Xdh*) and *PSI P700 apoprotein A2* (*PsaB*); Table S4) for a total of 8823 aligned nucleotides, and analysed it by ML as described above, with the GTR + G model with six gamma rate categories and seven data partitions. This resolved the Vanilloideae as sister to Cypripedoideae, Orchidoideae and Epidendroideae with 100% bootstap support (see Fig. 5 later). In subsequent analyses, Vanilloideae were therefore constrained as sister to Cypripedioideae, Orchidoideae and Epidendroideae.

Molecular clock dating relied on the uncorrelated lognormal relaxed clock model implemented in BEAST v. 1.7 (Drummond *et al.*, 2012). We used the same model of nucleotide substitution as before, a Yule tree prior, and a Markov chain Monte Carlo (MCMC) chain length of 100 million generations, sampling every 10 000 generations. Four fossil calibrations were used. The oldest known fossil of the Asparagales (105 million yr; Walker & Walker, 1984) was used as a maximal calibration point for the Orchidaceae, following (Gustafsson *et al.*, 2010), and was given a large normal prior (offset = 105.3; SD = 8). A gamma distribution was used on each of the three ingroup fossil constraints (the offset value was set to the minimum age of each fossil and the standard deviation was set such that the maximum age was included in the 97.5% quantile). The fossil orchid *Meliochis*

caribea (15–20 million yr; Ramírez *et al.*, 2007) was used as a minimal constraint for the monophyletic tribe Goodyerinae, under a gamma prior (offset = 17.5; SD = 5). Two recently discovered orchid macrofossils (*Dendrobium winkaphyllum* and *Earina fouldenensis*; both 20–23 million yr; Conran *et al.*, 2009) were used as minimum constraints within Epidendroideae, with gamma priors (offset = 20; SD = 4.5). The trees were summarized using TreeAnnotator v. 1.8.0 (part of the BEAST package), with a 10% burn-in and a 0.98 posterior probability limit.

Ancestral habit reconstruction

Using local floras and photographs, the 340 taxa were coded as terrestrial (0) or epiphytic (1) (Fig. S5). Ancestral reconstruction relied on the chronogram and an asymmetric two-rate Markov parameter model (Lewis, 2001) as implemented in Mesquite (Maddison & Maddison, 2011). This model assumes that gains and losses of epiphytism may have different probabilities.

Results

Flavonoids localize in the velamen of epiphytic orchids

To determine whether the velamen could be involved in UV-B photoprotection, we localized flavonoids in the roots of five species selected to represent orchid phylogenetic and habit diversity, using DPBA staining (Fig. 1). Accumulation of flavonoids in the velamen occurred only in species with aerial photosynthetic roots (*V. planifolia*, *D. lindenii* and *A. giganteum*; Fig. 1). By contrast, flavonoids were absent from the velamen of the terrestrial orchid *C. kentuckiense* and the rhizodermis of *D. fuchsii*, which lacks a velamen (Fig. 1b,c). Moreover, in *D. lindenii*, a leafless epiphytic species with flattened roots, stronger flavonoid fluorescence was present in the upper (exposed) side as compared to the lower side of the root (Fig. 1d). Flavonoids accumulated strongly in living velamen cells of light-exposed *Phalaenopsis* × *hybrida* root apices, and dark-grown roots accumulated very weak flavonoid fluorescence (Fig. S1). Taken together, these findings suggest that flavonoid localization in the velamen is light inducible and associated with the epiphytic habit and that it is synthesized in the root apex, before velamen maturation.

Two flavone glucosides absorb UV-B radiation, resulting in the maintenance of high photosynthetic efficiency in roots under UV-B stress

To probe whether the flavonoids are induced by UV-B radiation itself, and to identify the flavonoids involved, we performed UV-B induction experiments followed by LC-MS analyses. UV-B treatment resulted in a rapid accumulation of flavonoids in the upper side of the root. Two flavone glucosides, saponarin ($m/z = 595$ $(M+H)^+$) and a vitexin glucoside ($m/z = 651$ $[M+H]^+$), showed a fivefold increase upon UV-B treatment (Fig. 2a). A smaller, but significant, increase in the concentration of saponarin in dark-grown roots indicated constitutive accumulation and that vitexin glucoside can be induced by white light. The absorbance spectra of both compounds (205–400 nm) encompassed the UV-B emission range (280–315 nm; Fig. 2b). To further probe the effectiveness of flavone glucosides in UV-B screening, we measured the photosynthetic efficiency of PSII by examining chlorophyll fluorescence in mature, light-grown roots before and after UV-B irradiation (see the Materials and Methods section). Values of F_v/F_m in UV-B-treated roots were high and similar to those in control roots (mean ± SE: 0.77 ± 0.03 and 0.78 ± 0.02 for control and UV-B treated roots, respectively), showing that flavone glucoside accumulation efficiently protects the photosynthetic root cortex against harmful UV-B radiation. Comparison of the flavonoid profiles of the root and full light-grown *Phalaenopsis* × *hybrida* leaves revealed a similar asymmetry in the two compounds (Fig. S2), indicating that the leaf-to-root function transfer of UV-B protection recruited the same metabolites.

Differential expression of chalcone synthase paralogues in *Phalaenopsis* × *hybrida* velamen

To investigate whether living (young) velamen cells act as a UV-B sensor and to determine the genetic basis of flavonoid up-regulation, we monitored the expression pattern of three paralogues of chalcone syntase (representing the two lineages identified by our phylogenetic analysis; Fig. 3a–c) in different parts of the roots under varying UV-B stress. After 4 h of UV-B treatment, the phylogenetically close *PhCHS3* and *PhCHS4* paralogues were up-regulated in the entire root tip, indicating a locally systemic response to UV-B radiation (Fig. 4a), consistent with a sensor role for the living velamen. *PhCHS4* was strongly up-regulated on the upper side of the roots after 8 and 12 h of UV-B treatment (15- and 12-fold, respectively) (Fig. 4b–c). Although, after 4 h of treatment, it seemed that *PhCHS5* was also up-regulated, the *PhCHS5* expression level was not correlated to the duration of UV-B radiation exposure (Fig. 4b–f). In mature roots, *PhCHS4* was highly up-regulated in the upper side of the root in the 4-, 8- and 12-h treatments, while *PhCHS3* showed weaker expression (Fig. 4d,e); *PhCHS5* was very weakly expressed regardless of the duration of UV-B exposure (Fig. 4d,e). In all experiments, expression was restricted to the upper, exposed side, and no expression change occurred in the lower side. To further characterize the differences in expression patterns, the log values for all expression experiments of the different *PhCHS* genes were plotted against one another. *PhCHS3* and *PhCHS4* expression showed a positive linear correlation, very strong in the mature root and weaker in the root tip (Fig. 4g), in both cases highly significant (Pearson's correlation coefficient 0.95 and 0.67, respectively; $P < 0.001$; Table S1 summarizes all correlation statistics), indicating that both genes are up-regulated in the root under UV-B stress. However, the expression of *PhCHS3* was low compared with *PhCHS4*, except at 4 h in the root tip, indicating that *PhCHS4* is the main *CHS* involved in flavonoid biosynthesis in the velamen. By contrast, no significant correlation was found between *PhCHS5* and either *PhCH3* or *PhCHS4* (Fig. 4h,i, Table S1). The weaker correlation of the expression of the latter two genes in the root tip reflects the local burst of *PhCHS3/4*

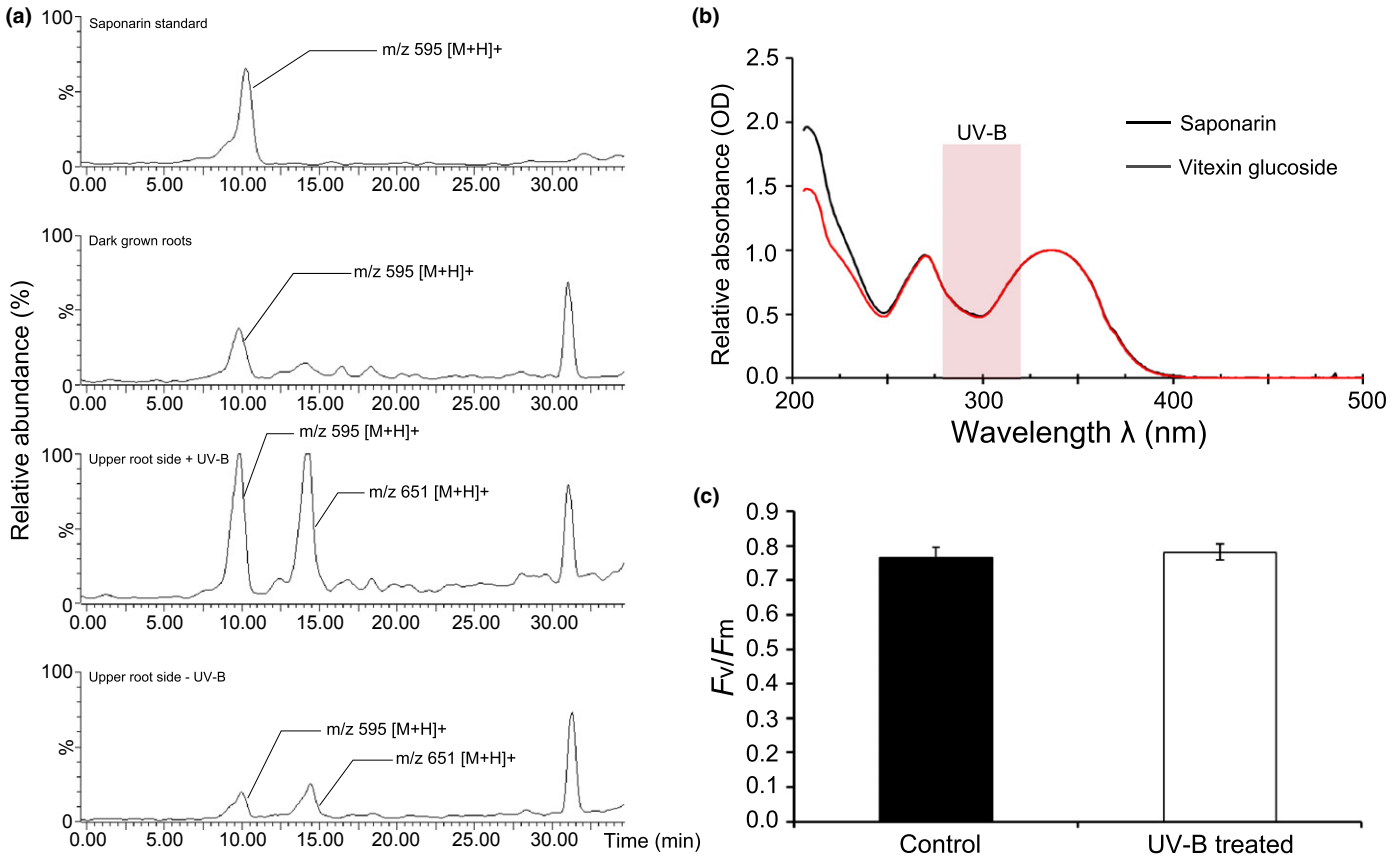

Fig. 2 Saponarin and isovitexin glucosides are induced by and absorb UV-B, protecting the root cortex from UV-B radiation. (a) Chromatogram of *Phalaenopsis* × *hybrida* root. (b) Absorbance spectra of the two glucosides, saponarin (black line) and vitexin glucoside (red line). (c) Photosynthetic efficiency of photosystem II (PSII) evaluated using chlorophyll fluorescence. $n = 3$ roots in each case; 10 measurements were made per root. Error bars, ± SE.

expression observed after 4 h of UV-B radiation and is consistent with a sensor role for the living velamen.

Duplication of chalcone synthase genes in orchids

We inferred a phylogeny of chalcone synthases from 148 CHS-like protein sequences, rooted on bryophyte CHSs (Figs 3a, S3). Two distinct orchid CHS clades were recovered with high statistical confidence (ML bootstrap support > 95) within the four (of five) subfamilies sampled (Fig. 3a–c). Both orchid CHS clades are present in the four orchid families sampled, with the exception of clade 2 in Cypripedioideae, probably as a consequence of under-sampling (a single sequence could be included in the analysis). The clade leading to the *PhCHS3/4* orchid CHS lineages has members in eudicots (Figs 3a, S3), indicating that the initial duplication of the two orchid CHS lineages predates the most recent common ancestor of eudicots and monocots, and may thus be > 140 million yr old (Davies *et al.*, 2004; Smith *et al.*, 2010).

Gains and losses of the epiphytic habit in orchids

To infer when and how many times root UV-B protection evolved and was lost, we generated a dated phylogeny of Orchidaceae, using 4.2 kb of plastid and nuclear DNA for 37% of the 899 orchid genera, calibrated with four fossil constraints (see the Materials and Methods section). This tree was used to reconstruct the evolution of the terrestrial and the epiphytic habits. To better resolve the ambiguous position of Vanilloideae and Cypripedioideae (Cameron *et al.*, 1999; Freudenstein & Chase, 2001; Freudenstein *et al.*, 2004; Górniak *et al.*, 2010), we enlarged a subset of the DNA matrix to 9 kb, which yielded a strong phylogenetic signal for Vanilloideae as sister to Cypripedioideae, Orchidoideae and Epidendroideae (ML bootstrap support = 100), and Cypripedioideae as sister to Orchidoideae and Epidendroideae (ML bootstrap support = 88) (Fig. 5). The chronogram implies that the most recent common ancestor of orchids lived in the Upper Cretaceous, 93.7 (121–75 Ma; 95% Highest Posterior Density (HPD)) million yr ago (Fig. 6).

Our ML ancestral state reconstruction suggests that epiphytism evolved a minimum of four to seven times over the past 43 million yr and was lost again at least seven to 10 times (Figs 6, S5). Although our ancestral state reconstruction probably indicates only the oldest gains and losses of epiphytism, it is likely that many more occurred more recently (more derived in the phylogeny), as implied by the occurrence of several epiphytic genera with one or a

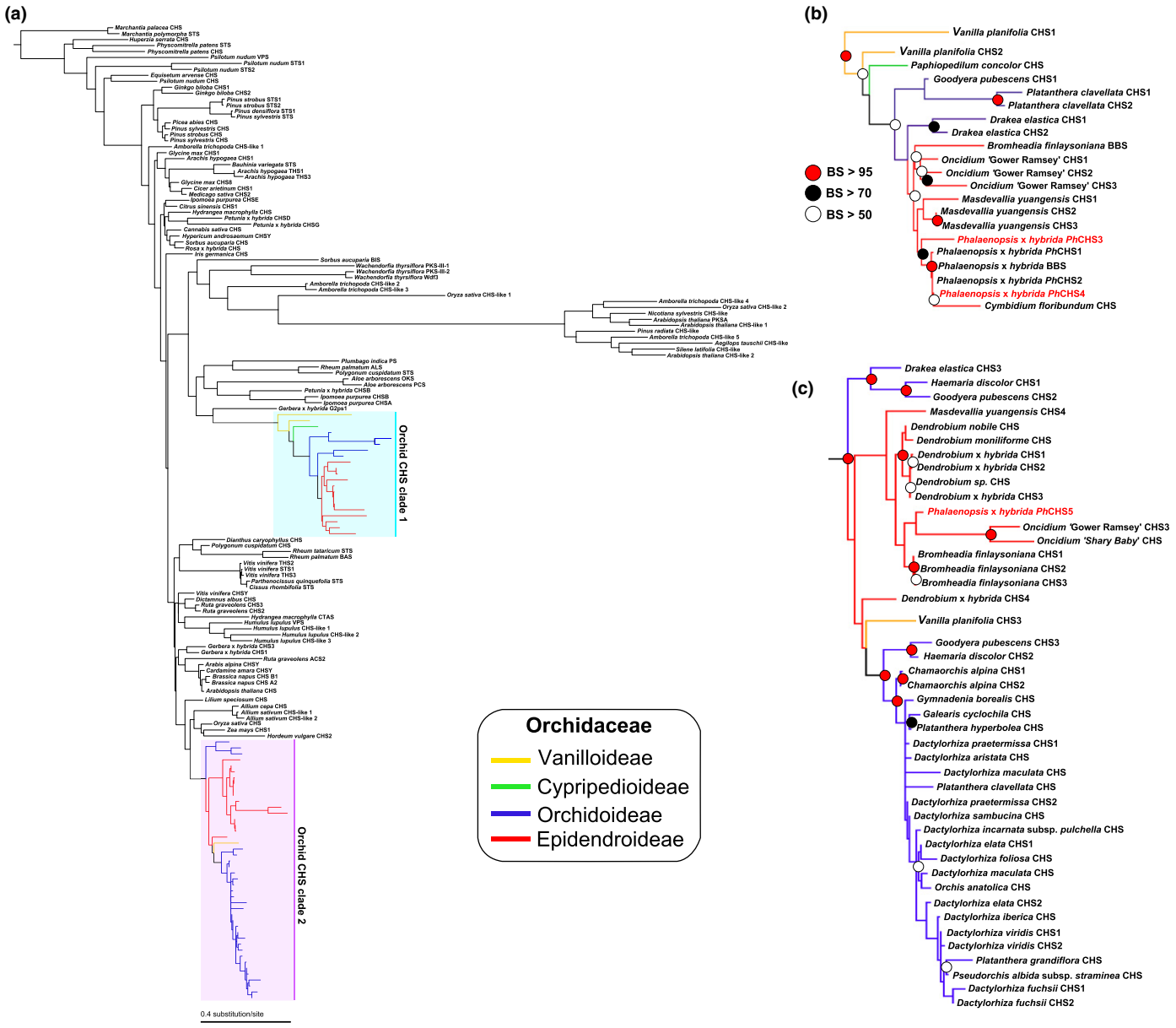

Fig. 3 Phylogenetic analysis of chalcone synthase (CHS) and related type III polyketide synthase proteins in land plants, showing the two lineages of orchid CHS. (a) Maximum likelihood phylogenetic tree for 147 CHS-like proteins spanning all land plants under a LG + G substitution model; the position of orchid CHS is shown. Color-coding of the branches is as follow: yellow, Vanilloideae; green, Cypripedioideae; blue, Orchidoideae; red, Epidendroideae. (b) Close-up of orchid CHS clade 1. (c) Close-up of orchid CHS clade 2. The studied CHSs are shown in red in (b) and (c). CHS, chalcone synthase; STS, stilbene synthase; VPS, valerophenone synthase; ALS, aloesone synthase; PS, pyrone synthase; PKS, polyketide synthase; THS, tri-hydrostilbene synthase; PCS, pentaketide chromone synthase; BAS, benzalacetone synthase; BIS, biphenyl synthase; OKS, octaketide synthase; CTAS, coumaroyl triacetic acid synthase; ACS, acridone synthase.

few terrestrial members (Zotz, 2013). The most recent common ancestors of each of the five subfamilies (Apostasioideae, Vanilloideae, Cypripedioideae, Orchidoideae and Epidendroideae) were inferred to be terrestrial (Fig. 6; ML probability > 95).

Discussion

The velamen functions in UV-B protection

The systemic up-regulation of *PhCHS3/4* in the entire root apex region is consistent with a sensor role for the living velamen. The ability of velamen cells to sense high-intensity damaging UV-B radiation is unique and contrasts with *A. thaliana* roots, which can only sense nondamaging low UV-B intensities (Tong *et al.*, 2008; Leasure *et al.*, 2009). Expression of *PhCHS3* and *PhCHS4* in the living velamen of the entire apical region would result in durable coating of the whole root by UV-B screening flavone glucosides. This is the first report and demonstration of the function of the velamen in UV-B protection, although it has previously been suggested that the velamen protects against an excess of solar radiation (Garay, 1972). The exodermis may also participate in UV-B

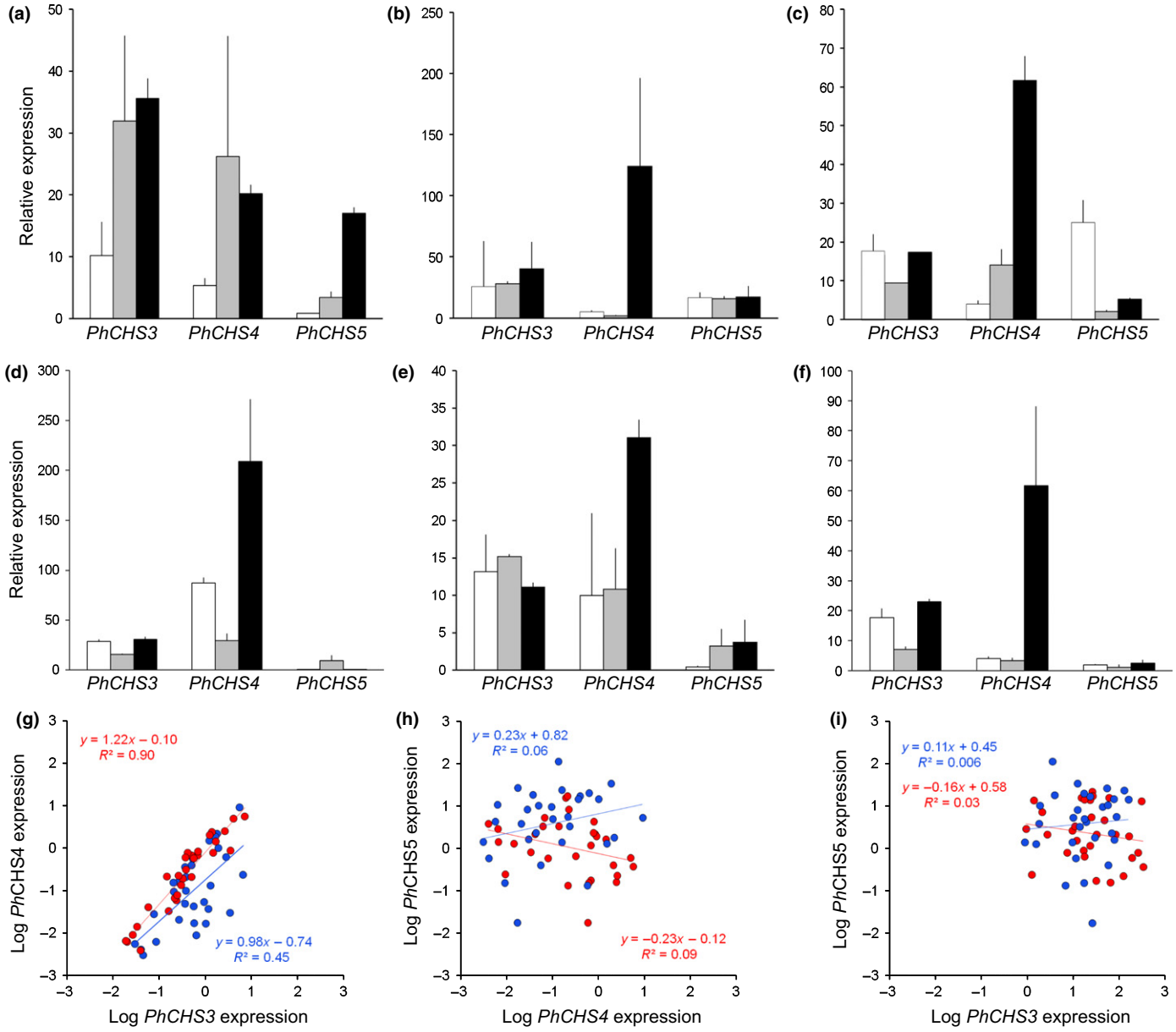

Fig. 4 UV-B induces *Phalaenopsis* × *hybrida* chalcone synthase (*CHS*) clade 1 genes *PhCHS3* and *PhCHS4* but not clade 2 *PhCHS5*. (a–c) *PhCHS* expression in root tips, (a) after 4 h of UV-B treatment, (b) after 8 h of UV-B treatment, and (c) after 12 h of UV-B treatment. (d–f) *PhCHS* expression in fully expanded, mature roots, (d) after 4 h of UV-B treatment, (e) after 8 h of UV-B treatment, and (f) after 12 h of UV-B treatment. (a–f) White bars, control; grey bars, lower root side + UV-B; black bars, upper root side + UV-B. (g–h) Linear regression of *PhCHS* expression across all experiments. (g) *PhCHS3* and *PhCHS4*. (h) *PhCHS4* and *PhCHS5*. (i) *PhCHS3* and *PhCHS5*. Error bars, ± SE of triplicates.

screening in some orchid species, but typically it accumulates phenolics constitutively, while the velamen is UV-B inducible (e.g. see Fig. 1; *Dendrophylax lindenii*). Whether the distinct behaviour of living velamen cells reflects a 'size effect' attributable to the smaller cell size in the root apical region (resulting in more cells receiving a UV-B signal for the same exposed surface) or an intrinsic physiological difference remains unclear. By contrast, the strong correlation of *PhCHS3* and *PhCHS4* expression in the mature root is consistent with a local response, indicating that the mature root can locally enhance its UV-B screen, by accumulating flavonoids in the next living cell layers, that is, the upper cortical layers, a phenomenon that occurs in leaves under strong UV-B radiation (Tattini *et al.*, 2000, 2005).

These results show that *PhCHS3* and *PhCHS4* are co-expressed under UV-B stress, while *PhCHS5* is not UV-B inducible. *PhCHS5* is strongly expressed in *Phalaenopsis* × *hybrida* flowers when anthocyanin accumulates, and it plays a role in flower pigmentation (Han *et al.*, 2006). Therefore, the distinct functions of the two *Phalaenopsis* × *hybrida CHS* lineages arose following an ancient duplication, predating the origin of epiphytic orchids by *c.* 100 million yr, which contrasts markedly with the recent *CHS* duplications and functional divergence in *Petunia* (Solanaceae) and *Ipomoea* (Convolvulaceae) (Koes *et al.*, 1989;

Fig. 5 Phylogenetic relationships among orchid subfamilies inferred from a seven-gene matrix (four chloroplastic (*rbcL*, *matK*, *trnL-trnF* and *PsaB*) and three nuclear (ITS, *18S* and *Xdh*)), totalling *c.* 9 kb aligned DNA. The two arrows show the nodes that had no or contradicting support in previous analyses. Bootstrap values are shown at nodes.

Durbin *et al.*, 1995, 2000). Whether sub- or neofunctionalization is involved in this case is unclear because of the lack of knowledge of the ancestral function, and the distinct functions of *PhCHS* clades 1 and 2 might in fact be attributable to *cis*-acting element evolution rather than protein functional divergence.

Comparison of root UV-B photoprotection with leaf epidermis photoprotection

Phenolic compounds, mostly flavonoids, have long been known to be involved in UV-B photoprotection in leaves (Caldwell *et al.*, 1983; Li *et al.*, 1993). Simpler phenolics, such as hydroxycinnamic acids (HCAs), also participate in UV-B screening, especially in young leaves (Burchard *et al.*, 2000), and the correlated decrease of HCAs and increase of flavonoids during ontogeny suggests that the former are redirected to the flavonoid pathway. Because epidermal cells are alive throughout the lifespan of a leaf, flavonoid concentrations can be adjusted to ambient UV-B intensities (Burchard *et al.*, 2000; Bidel *et al.*, 2007). In the *Phalaenopsis* × *hybrida* velamen, we did not find high concentrations of HCAs during our preliminary analyses (see the Materials and Methods section), suggesting that flavonoids, rather than simpler phenolics, are directly accumulated as UV-B screening compounds. In contrast to the epidermis, the orchid velamen, much like xylem cells, is functional as a dead tissue and probably matures following programmed cell death. While UV-B-mediated flavonoid accumulation in leaves typically occurs in a local, nonsystemic way in leaves (Bidel *et al.*, 2007; L. P. R. Bidel *et al.*, unpublished), we showed that, in the *Phalaenopsis* × *hybrida* velamen, it occurs by systemic expression of *PhCHS3/4* in living velamen cells, thus permitting rapid flavonoid accumulation during the short lifespan of velamen cells (1–2 wk). Modulation of the flavonoid concentration in the mature velamen is not possible, but increased in the expression of *PhCHS4* and histology shows that flavonoids can be accumulated in the exodermal cells or the closest mesophyll cells (Figs 4d–f, S1), similarly to deeper flavonoid accumulation in leaves exposed to high light intensities (Tattini *et al.*, 2000, 2005). Thus, UV-B protection in the velamen is fundamentally different from that in epidermises.

Cenozoic gains and losses of the epiphytic habit mirror the evolution of root UV-B photoprotection

Our Upper Cretaceous age for the crown group of Orchidaceae (93.7 (121–75) million yr; 95% HPD) overlaps the range found in a previous dating analysis (Janssen & Bremer, 2004) but is older than that found in two more local analyses (Ramírez *et al.*, 2007: 58 taxa and two fossil constraints; Gustafsson *et al.*, 2010: 58 taxa and four constraints). The Cenozoic radiation of epiphytic orchids was contemporaneous with that of epiphytic leptosporangiate ferns (Schuettpelz & Pryer, 2009), suggesting that the establishment of modern rainforests drove epiphyte radiations at that time. As outlined in this study, root UV-B protection requires root UV-B-inducible chalcone synthase and an anatomical structure that can accumulate flavonoids in high quantities. It is unlikely that ancestral clade 1 chalcone synthases in early orchids were involved in root UV-B photoprotection, given these orchids' inferred terrestrial habit (Fig. 6); instead, it is likely that clade 1 chalcone synthases were only later co-opted for root UV-B protection. Consistent with this idea, the *Gerbera hybrida G2PS1* (*Gerbera hybrida* 2-pyrone synthase) gene, sister to all orchid clade 1 *CHS* genes in our tree (Figs 3a, S3), is functionally divergent from *CHS* and encodes a 2-pyrone synthase (Deng *et al.*, 2014). Whether the different lineages of epiphytes independently co-opted CHS clade 1 to function in root photoprotection or whether it was recruited from leaf UV-B protection is unclear. However, the similarity of leaf and root flavonoid patterns in *Phalaenopsis* × *hybrida* (Figs 2, S2) suggests a leaf-to-root function transfer rather than a co-option.

The second ingredient needed for root UV-B protection is a structure capable of accumulating large amounts of flavonoids,

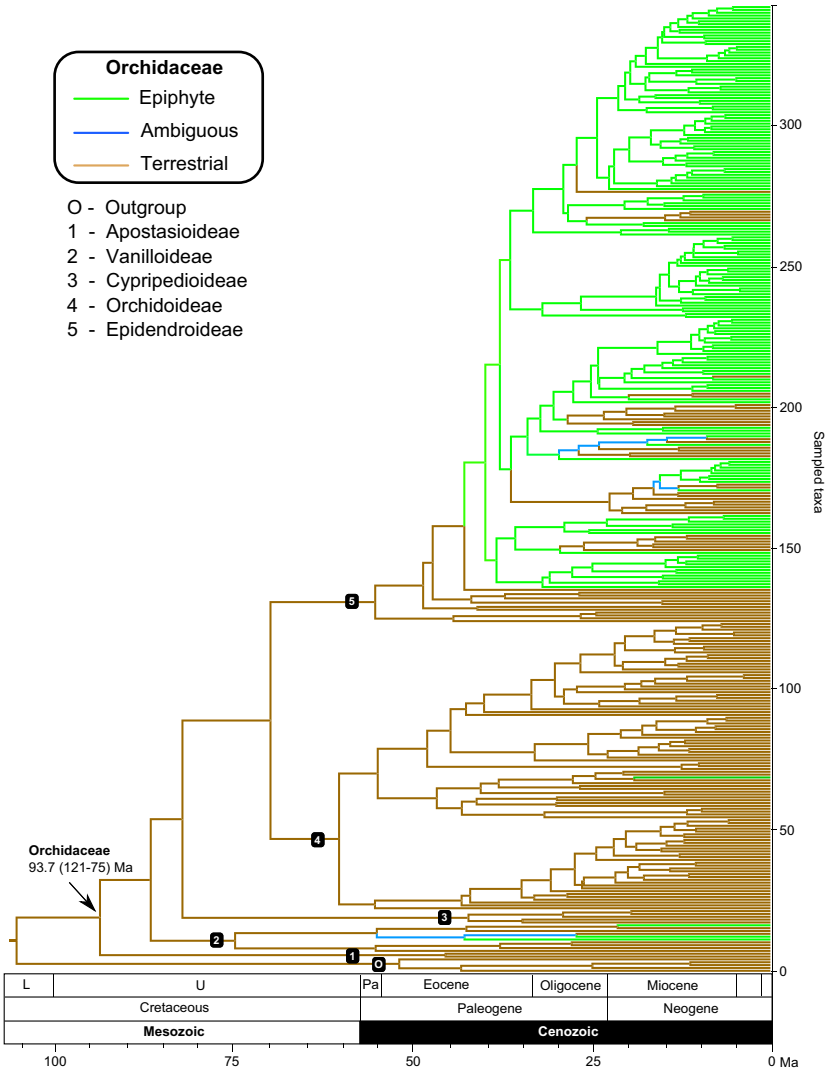

Fig. 6 Orchidaceae time tree, on which habit evolution has been reconstructed by maximum likelihood (ML) under a two-rate asymmetric Markov model. Ancestral state is considered ambiguous (blue) when the ML probability ratio is below 70/30 for the two states. Ma, million yr ago.

such as a velamen. Apostasioideae, Vanilloideae, some Cypripedioideae, and all epiphytic Epidendroideae studied have a velamen (Porembski & Barthlott, 1988; Judd *et al.*, 1993), suggesting that the presence of a velamen is the ancestral state in Orchidaceae, while lack of a velamen would reflect a secondary (apomorphic) loss. Although we cannot infer the pattern of velamen evolution because of the limited knowledge of orchid root anatomy across the family's phylogeny, secondary returns to the terrestrial habit in Epidendroideae are in some cases associated with loss or reduction of the velamen (e.g. in *Govenia* and *Wullschlaegelia*; Stern & Judd, 2002; Stern & Carlsward, 2008; our Figs 6, S5). Thus, the UV-B protective function of epiphytic orchid roots is the result of the evolution of both *CHS* gene regulation and the velamen structure itself; when lineages returned to a ground-dwelling habit, the protective function was probably lost again.

A study of 345 orchid species covering the five subfamilies revealed that 40% of the 40 included terrestrial Orchidoideae lack a velamen (Porembski & Barthlott, 1988; Figs 1, 6). Terrestrial orchids typically have a cortex fully infested by mycorrhizal pelotons while epiphytic orchids often show weaker levels of infection (Zelmer *et al.*, 1996; Otero *et al.*, 2002; Fig. 1c). Flavonoid-rich velamen and exodermal cell walls are an important barrier to fungal hyphae, which can only enter the cortex through flavonoid-poor exodermal passage cells (Esnault *et al.*, 1994; Chomicki *et al.*, 2014). Thus, stronger dependence on mutualistic fungi probably favoured a reduction of root flavonoids and degradation of the velamen, as observed in many Orchidoideae and myco-heterotrophic Epidendroideae (Gastrodieae and Neottieae; Porembski & Barthlott, 1988).

Conclusions

The *velamen radicum* of epiphytic orchids has long been thought to play a key role in water and nutrient absorption and storage (Went, 1940), although experimental demonstration of this came more recently (Capesius & Barthlott, 1975; Zotz & Winkler, 2013). Using an integrative approach, we showed that it also plays a pivotal role in UV-B protection. This is achieved by a UV-B induced systemic up-regulation of specific chalcone

synthase paralogues in living velamen cells of the root tip, leading to the accumulation of two flavone glycosides in the cell walls, which in turn provides long-lasting protection against UV-B damage that persists well after the death of the velamen cells. Although flavonoids have long been known to be essential players in UV-B protection in leaf and other epidermises, the mechanism demonstrated here is unique in that it involves rapid flavonoid induction in young cells followed by binding to the cell walls before programmed cell death. Some 300 species of epiphytic orchids are leafless and rely exclusively on root photosynthesis (Chomicki *et al.*, 2014), possibly as an adaptation to frequent or extreme droughts in their habitats (Benzing *et al.*, 1983). The partial or total transfer of the carbon gain function to roots probably participates in the reduction of the plant surface to volume ratio (as roots have a lower surface to volume ratio than leaves). Thus, the described UV-B protection function of orchid roots is an essential adaptation to the water-limited epiphytic habit. Based on our time-calibrated orchid phylogeny, the multifunctionality of the orchid velamen probably contributed to the family's expansion into rainforest canopies during the Cenozoic.

Acknowledgements

We thank the Ministry of Agriculture of China (grant no. 2008ZX08009-001-008) and the Natural Science Foundation of Shanghai (grant No. 12ZR1402300) for funding. The 1KP project is acknowledged for permission to use a few orchid CHS. The American Society of Plant Biology is thanked for a travel grant award to G.C. in 2012. Jeremy Aroles is thanked for editing of the manuscript. For discussion, we thank Tom Givnish and Robert Ricklefs. We thank the Editor Elena Kramer and three anonymous reviewers for constructive comments on the manuscript.

References

Benzing DH, ed. 2000. *Bromeliaceae: profile of an adaptive radiation.* Cambridge, UK: Cambridge University Press.

Benzing DH. 2008. *Vascular epiphytes: general biology and related biota.* New York, NY, USA: Cambridge University Press.

Benzing DH, Friedman WE, Peterson G, Renfrow A. 1983. Shootlessness, velamentous roots, and the pre-eminence of Orchidaceae in the epiphytic biotope. *American Journal of Botany* **70**: 121–133.

Bidel LPR, Meyer S, Goulas Y, Cadot Y, Cerovic ZG. 2007. Responses of epidermal phenolic compounds to light acclimation: *in vivo* qualitative and quantitative assessment using chlorophyll fluorescence excitation spectra in leaves of three woody species. *Journal of Photochemistry and Photobiology B* **88**: 163–179.

Bray CM, West CE. 2005. DNA repair mechanisms in plants: crucial sensors and effectors for the maintenance of genome integrity. *New Phytologist* **168**: 511–528.

Burchard P, Bilger W, Weissenböck G. 2000. Contribution of hydroxycinnamates and flavonoids to epidermal shielding of UV-A and UV-B radiation in developing rye primary leaves as assessed by ultraviolet-induced chlorophyll fluorescence measurements. *Plant, Cell & Environment* **23**: 1373–1380.

Caldwell MM, Robberecht R, Flint SD. 1983. Internal filters: prospects for UV-acclimation in higher plants. *Physiology Plantarum* **58**: 445–450.

Cameron KM, Chase MW, Whitten WM, Kores PJ, Jarrell DC, Albert VA, Yukawa T, Hills HG, Goldman DH. 1999. A phylogenetic analysis of the Orchidaceae: evidence from rbcL nucleotide sequences. *American Journal of Botany* **86**: 208–224.

Canham CD, Denslow JS, Platt WJ, Runkle JR, Spies TA, White PS. 1990. Light regimes beneath closed canopies and tree-fall gaps in temperate and tropical forests. *Canadian Journal of Forest Research* **20**: 620–631.

Capesius I, Barthlott W. 1975. Isotopen-Markierungen and Rasterelektronenmikroskopische Untersuchungen am Velamen radicum der Orchideen: Isotope labelling and scanning electron microscope studies of the velamen radicum of Orchideen. *Zeitschrift für Pflanzenphysiologie* **75**: 436–448.

Castresana J. 2000. Selection of conserved blocks from multiple alignments for their use in phylogenetic analysis. *Molecular Biology and Evolution* **17**: 540–552.

Chomicki G, Bidel LPR, Jay-Allemand C. 2014. Exodermis structure controls fungal invasion in the leafless epiphytic orchid *Dendrophylax lindenii* Lindl. Benth. ex Rolfe. *Flora* **209**: 88–94.

Cockburn W, Goh CJ, Avadhani PN. 1985. Photosynthetic carbon assimilation in a shootless orchid, *Chiloschista usneoides* Don. LDL a variant on Crassulacean Acid Metabolism. *Plant Physiology* **77**: 83–86.

Conran JG, Bannister JM, Lee DE. 2009. Earliest orchid macrofossils: early Miocene *Dendrobium* and *Earina* Orchidaceae: Epidendroideae from New Zealand. *American Journal of Botany* **96**: 466–474.

Crayn DM, Winter K, Smith JAC. 2004. Multiple origins of crassulacean acid metabolism and the epiphytic habit in the Neotropical family Bromeliaceae. *Proceedings of the National Academy of Sciences, USA* **101**: 3703–3708.

Darriba D, Taboada GL, Doallo R, Posada D. 2011. ProtTest 3: fast selection of best-fit models of protein evolution. *Bioinformatics* **27**: 1164–1165.

Davies TJ, Barraclough TG, Chase MW, Soltis PS, Soltis DE, Savolainen V. 2004. Darwin's abominable mystery: insights from a supertree of the angiosperms. *Proceedings of the National Academy of Sciences, USA* **101**: 1904–1909.

Deng X, Bashandy H, Ainasoja M, Kontturi J, Pietiäinen M, Laitinen RAE, Albert VA, Valkonen J, Elomaa P, Teeri TH. 2014. Functional diversification of duplicated chalcone synthase genes in anthocyanin biosynthesis of *Gerbera hybrida*. *New Phytologist* **201**: 1469–1483.

Drummond AJ, Suchard MA, Xie D, Rambaut A. 2012. Bayesian phylogenetics with BEAUti and the BEAST 1.7. *Molecular Biology and Evolution* **29**: 1969–1973.

Durbin ML, Learn GH, Huttley GA, Clegg MT. 1995. Evolution of the chalcone synthase gene family in the genus *Ipomoea*. *Proceedings of the National Academy of Sciences, USA* **92**: 3338–3342.

Durbin ML, McCaig B, Clegg MT. 2000. Molecular evolution of the chalcone synthase multigene family in the morning glory genome. *Plant Molecular Biology* **42**: 79–92.

Esnault AL, Masuhara G, McGee PA. 1994. Involvement of exodermal passage cells in mycorrhizal infection of some orchids. *Mycological Research* **98**: 672–676.

Flint SD, Caldwell MM. 1998. Solar UV-B and visible radiation in tropical forest gaps: measurements partitioning direct and diffuse radiation. *Global Change Biology* **4**: 863–870.

Freudenstein JV, Chase MW. 2001. Analysis of mitochondrial nad1 bc intron sequences in Orchidaceae: utility and coding of length-change characters. *Systematic Botany* **26**: 643–657.

Freudenstein JV, van den Berg C, Goldman DH, Kores PJ, Molvray M, Chase MW. 2004. An expanded plastid DNA phylogeny of Orchidaceae and analysis of jackknife branch support strategy. *American Journal of Botany* **91**: 149–157.

Garay LA. 1972. On the origin of the Orchideaceae 2. *Journal of the Arnold Arboretum* **53**: 202–215.

Gay H. 1993. Animal-fed plants: an investigation into the uptake of ant-derived nutrients by the far-eastern epiphytic fern *Lecanopteris* Reinw. Polypodiaceae. *Biological Journal of the Linnean Society* **50**: 221–233.

Gegenbauer C, Mayer VE, Zotz G, Richter A. 2012. Uptake of ant-derived nitrogen in the myrmecophytic orchid *Caularthron bilamellatum*. *Annals of Botany* **110**: 757–766.

Givnish TJ, Barfuss MHJ, Van Ee B, Riina R, Schulte K, Horres R, Gonsiska PA, Jabaily RS, Crayn DMF, Smith JAC *et al.* 2014. Adaptive radiation, correlated and contingent evolution, and net species diversification in Bromeliaceae. *Molecular Phylogenetics and Evolution* **71**: 55–78.

Górniak M, Paun O, Chase MW. 2010. Phylogenetic relationships within Orchidaceae based on a low-copy nuclear coding gene Xdh: congruence with organellar and nuclear ribosomal DNA results. *Molecular Phylogenetics and Evolution* **56**: 784–795.

Gustafsson ALS, Verola CF, Antonelli A. 2010. Reassessing the temporal evolution of orchids with new fossils and a Bayesian relaxed clock, with implications for the

diversification of the rare South American genus *Hoffmannseggella* Orchidaceae: Epidendroideae. *BMC Evolutionary Biology* **10**: 177.

Han YY, Ming F, Wang W, Wang JW, Ye MM, Shen DL. 2006. Molecular evolution and functional specialization of chalcone synthase superfamily from *Phalaenopsis* Orchid. *Genetica* **128**: 429–438.

Huxley CR. 1978. The ant-plants *Myrmecodia* and *Hydnophytum* Rubiaceae, and the relationships between their morphology, ant occupants, physiology and ecology. *New Phytologist* **80**: 231–268.

Jansen MA, Gaba V, Greenberg BM. 1998. Higher plants and UV-B radiation: balancing damage, repair and acclimation. *Trends in Plant Science* **3**: 131–135.

Janssen T, Bremer K. 2004. The age of major monocot groups inferred from 800+ rbcL sequences. *Botanical Journal of the Linnean Society* **146**: 385–398.

Judd WS, Stern WL, Cheadle VI. 1993. Phylogenetic position of *Apostasia* and *Neuwiedia* Orchidaceae. *Botanical Journal of the Linnean Society* **113**: 87–94.

Katoh K, Standley DM. 2013. MAFFT multiple sequence alignment software version 7: improvements in performance and usability. *Molecular Biology and Evolution* **30**: 772–780.

Koes RE, Spelt CE, Mol JN. 1989. The chalcone synthase multigene family of *Petunia hybrida* V30.: differential, light-regulated expression during flower development and UV light induction. *Plant Molecular Biology* **12**: 213–225.

Kwok-ki H, Hock-Hin Y, Choy-Sin H. 1983. The presence of photosynthetic machinery in aerial roots of leafy orchids. *Plant & Cell Physiology* **24**: 1317–1321.

Laube S, Zotz G. 2003. Which abiotic factors limit vegetative growth in a vascular epiphyte? *Functional Ecology* **17**: 598–604.

Leasure CD, Tong H, Yuen G, Hou X, Sun X, He ZH. 2009. Root UV-B sensitive2 acts with root UV-B sensitive1 in a root ultraviolet B-sensing pathway. *Plant Physiology* **150**: 1902–1915.

Lewis PO. 2001. A likelihood approach to estimating phylogeny from discrete morphological character data. *Systematic Biology* **50**: 913–925.

Li J, Ou-Lee TM, Raba R, Amundson RG, Last RL. 1993. *Arabidopsis* flavonoid mutants are hypersensitive to UV-B irradiation. *Plant Cell* **5**: 171–179.

Livak KJ, Schmittgen TD. 2001. Analysis of relative gene expression data using real-time quantitative PCR and the $2^{-\Delta\Delta CT}$ method. *Methods* **25**: 402–408.

Maddison WP, Maddison DR. 2011. *Mesquite 2.75: a modular system for evolutionary analysis.* [WWW document] URL http://mesquiteproject.org [accessed 1 June 2014].

Otero JT, Ackerman JD, Bayman P. 2002. Diversity and host specificity of endophytic *Rhizoctonia*-like fungi from tropical orchids. *American Journal of Botany* **89**: 1852–1858.

Porembski S, Barthlott W. 1988. Velamen radicum micromorphology and classification of Orchidaceae. *Nordic Journal of Botany* **8**: 117–137.

Ramírez SR, Gravendeel B, Singer RB, Marshall CR, Pierce NE. 2007. Dating the origin of the Orchidaceae from a fossil orchid with its pollinator. *Nature* **448**: 1042–1045.

Schuettpelz E, Pryer KM. 2009. Evidence for a Cenozoic radiation of ferns in an angiosperm-dominated canopy. *Proceedings of the National Academy of Sciences, USA* **106**: 11200–11205.

Sheahan JJ, Rechnitz GA. 1992. Flavonoid-specific staining of *Arabidopsis thaliana*. *BioTechniques* **13**: 880–883.

Silvera K, Santiago LS, Cushman JC, Winter K. 2009. Crassulacean acid metabolism and epiphytism linked to adaptive radiations in the Orchidaceae. *Plant Physiology* **149**: 1838–1847.

Sinha RP, Häder DP. 2002. UV-induced DNA damage and repair: a review. *Photochemical & Photobiological Sciences* **1**: 225–236.

Smith SA, Beaulieu JM, Donoghue MJ. 2010. An uncorrelated relaxed-clock analysis suggests an earlier origin for flowering plants. *Proceedings of the National Academy of Sciences, USA* **107**: 5897–5902.

Smith SA, Dunn CW. 2008. Phyutility: a phyloinformatics tool for trees, alignments and molecular data. *Bioinformatics* **24**: 715–716.

Stamatakis A, Hoover P, Rougemont J. 2008. A rapid bootstrap algorithm for the RAxML web servers. *Systematic Biology* **57**: 758–771.

Stern WL, Carlsward BS. 2008. Vegetative anatomy of Calypsoeae (Orchidaceae). *Lankesteriana* **8**: 105–112.

Stern WL, Judd WS. 2002. Systematic and comparative anatomy of Cymbidieae (Orchidaceae). *Botanical Journal of the Linnean Society* **139**: 1–27.

Tattini M, Gravano E, Pinelli P, Mulinacci N, Romani A. 2000. Flavonoids accumulate in leaves and glandular trichomes of *Phillyrea latifolia* exposed to excess solar radiation. *New Phytologist* **148**: 69–77.

Tattini M, Guidi L, Morassi-Bonzi L, Pinelli P, Remorini D, Degl'Innocenti E, Giordano C, Massai R, Agati G. 2005. On the role of flavonoids in the integrated mechanisms of response of *Ligustrum vulgare* and *Phillyrea latifolia* to high solar radiation. *New Phytologist* **167**: 457–470.

Tong H, Leasure CD, Hou X, Yuen G, Briggs W, He ZH. 2008. Role of root UV-B sensing in *Arabidopsis* early seedling development. *Proceedings of the National Academy of Sciences, USA* **105**: 21039–21044.

Walker JW, Walker AG. 1984. Ultrastructure of Lower Cretaceous angiosperm pollen and the origin and early evolution of flowering plants. *Annals of the Missouri Botanical Garden* **71**: 464–521.

Went FW. 1940. Soziologie der Epiphyten eines tropischen Urwaldes. *Annales du Jardin Botanique de Buitenzorg* **50**: 1–98.

Winter K, Wallace BJ, Stocker GC, Roksandic Z. 1983. Crassulacean acid metabolism in Australian vascular epiphytes and some related species. *Oecologia* **57**: 129–141.

Zelmer CD, Cuthbertson L, Currah RS. 1996. Fungi associated with terrestrial orchid mycorrhizas, seeds and protocorms. *Mycoscience* **37**: 439–448.

Zotz G. 2013. The systematic distribution of vascular epiphytes–a critical update. *Botanical Journal of the Linnean Society* **171**: 453–481.

Zotz G, Winkler U. 2013. Aerial roots of epiphytic orchids: the velamen radicum and its role in water and nutrient uptake. *Oecologia* **171**: 733–741.

Supporting Information

Additional supporting information may be found in the online version of this article.

Fig. S1 DPBA staining of light- and dark-grown *Phalaenopsis* × *hybrida* roots.

Fig. S2 Chromatogram showing the flavonoid profile of *Phalaenopsis* × *hybrida* leaves.

Fig. S3 Maximum likelihood CHS phylogram with accession numbers.

Fig. S4 Maximum likelihood phylogram for the Orchidaceae.

Fig. S5 Dated phylogeny for the Orchidaceae, with all tips named.

Table S1 Statistics for the correlation of *Phalaenopsis* × *hybrida* chalcone synthase expression patterns

Table S2 Primers used for qRT-PCR of *Phalaenopsis* × *hybrida* chalcone synthase genes

Table S3 GenBank accession numbers for orchid sequences

Table S4 GenBank accession numbers for the small phylogeny to resolved the position of Cypripedioideae and Vanilloideae

Please note: Wiley Blackwell are not responsible for the content or functionality of any supporting information supplied by the authors. Any queries (other than missing material) should be directed to the *New Phytologist* Central Office.